

A *BEPPoSAX* STUDY OF THE PULSATING TRANSIENT X0115+63: THE FIRST X-RAY SPECTRUM WITH FOUR CYCLOTRON HARMONIC FEATURES

A. SANTANGELO,¹ A. SEGRETO,¹ S. GIARRUSSO,¹ D. DAL FIUME,² M. ORLANDINI,² A. N. PARMAR,³
T. OOSTERBROEK,³ T. BULIK,⁴ T. MIHARA,⁵ S. CAMPANA,⁶ G. L. ISRAEL,⁷ AND L. STELLA⁷

Received 1999 April 27; accepted 1999 July 12; published 1999 August 17

ABSTRACT

The recurrent hard pulsating X-ray transient X0115+63 was observed with *BeppoSAX* on 1999 March 19, when the source was at a 2–10 keV flux level of ~ 310 mcrab. We report on the high-energy spectrum of the source, concentrating on cyclotron resonant scattering features. The spectrum is strongly pulse phase dependent, and absorption features are detected at virtually all phases. In particular, four absorption-like features at 12.74, 24.16, 35.74, and 49.5 keV are observed in the descending edge of the main peak of the pulse profile. The ratios between the centroid energies of the lines with respect to the first are 1 : (1.9) : (2.8) : (3.9). These values are close to the harmonic relation expected from cyclotron resonant scattering in a strong magnetic field when relativistic effects are taken into account. The equivalent widths of the second, third, and fourth harmonics are found to be larger than that of the first harmonic, confirming the key role of two-photon processes in the spectral formation. These results provide the first evidence for *four harmonically spaced lines* in the spectrum of an accreting X-ray pulsar, yielding the clearest confirmation to date of their magnetic origin.

Subject headings: binaries: close — pulsars: individual (X0115+634) — stars: neutron — X-rays: stars

1. INTRODUCTION

Cyclotron features provide a powerful tool for directly measuring the high ($B \geq 10^{12}$ G) magnetic field strengths of accreting neutron stars in X-ray binaries. Because the electron cyclotron energy is $E_{\text{cyc}} = 11.6B_{12}$ keV, where B_{12} is the magnetic field strength in units of 10^{12} G, these features are expected to be observed at hard X-ray energies. Absorption-like features interpreted as cyclotron resonant scattering were first discovered in the spectrum of the low-mass X-ray binary pulsar Her X-1 (Trümper et al. 1978) and, subsequently, in the hard X-ray transient pulsar X0115+63 (Wheaton et al. 1979). Since then, cyclotron features have been detected in other X-ray binary pulsars with *Ginga* (Mihara 1995), HEXE/TTM on *Mir* (Kendziorra et al. 1994), OSSE on board *Compton Gamma-Ray Observatory* (*CGRO*; Grove et al. 1995), and, more recently, with *Rossi X-Ray Timing Explorer* (*RXTE*; Kreykenbohm et al. 1998) and *BeppoSAX* (Dal Fiume et al. 1999; Santangelo et al. 1999).

Relatively little is known on higher cyclotron harmonics. Besides the pioneering detection of two lines in the spectrum of X0115+63 (White, Swank, & Holt 1983), the presence of two cyclotron lines has been reported for Vela X-1 (Kreykenbohm et al. 1998; Orlandini et al. 1998), 4U 1907+09 (Cusumano et al. 1998; Santangelo et al. 1999), and A0535+26 (Kendziorra et al. 1994). Some of these detections are still to be confirmed.

X0115+63 is one of the best-studied X-ray transients (Rapaport et al. 1978). The source shows pulsation at ~ 3.6 s while orbiting an O9e companion (V635 Cassiopeiae; Unger et al. 1998) with a period of 24.3 days. As customary for this class of X-ray binaries, the X-ray continuum has been modeled with a power law with an exponential cutoff at high energies and photoelectric absorption at low energies (White, Swank, & Holt 1983; Nagase et al. 1991). Wheaton et al. (1979), using *HEAO 1 A-1*, first reported the discovery of an absorption line at ~ 20 keV. Based on *HEAO 1 A-2* data, White, Swank, & Holt (1983) detected cyclotron lines at ~ 11.5 and ~ 23 keV that appeared to be in absorption at the pulse peak and in emission during the interpulse. By interpreting the two lines in terms of the first and second harmonics of cyclotron resonant scattering, they derived $B \simeq 1 \times 10^{12}$ G. During the 1990 February outburst, observations with the Large Area Counter on board *Ginga* revealed absorption features at ~ 12 and ~ 23 keV for all pulse phases; an investigation of the X-ray spectrum up to 60 keV did not yield any evidence for higher harmonics (Nagase et al. 1991; Tamura et al. 1992).

On 1999 February 22 the BATSE instrument on board the *CGRO* satellite revealed the onset of another outburst of X0115+63 (Wilson, Harmon, & Finger 1999). *BeppoSAX* observed the source with its Narrow Field Instruments (NFIs) on four occasions: 1999 March 6, 19, 22, and 26. The data presented in this Letter are from the March 19 observation, when, shortly after the outburst maximum, the source was at a flux level of ~ 310 mcrab. These data led to the discovery of a four-harmonic cyclotron line spectrum in X0115+63, the first ever from a cosmic X-ray source. Our results predate the announcement of the discovery of the third cyclotron line in the spectrum of X0115+63 based on *RXTE*/HEXTE measurements (Heindl et al. 1999); therefore, they provide also an important independent confirmation of the latter result.

2. OBSERVATIONS AND SPECTRAL ANALYSIS

Besides the Low-Energy Concentrator Spectrometer (LECS; 0.1–10 keV; Parmar et al. 1997) and the Medium-Energy Concentrator Spectrometer (MECS; 2–10 keV; Boella et al. 1997b),

¹ Istituto Fisica Cosmica e Applicazioni all'Informatica (IFCAI), C. N. R. Via La Malfa 153, 90146 Palermo, Italy.

² Istituto Tecnologie e Studio Radiazioni Extraterrestri (TeSRE), C. N. R. Via Gobetti 101, 40129 Bologna, Italy.

³ Astrophysics Division, Space Science Department of ESA, ESTEC, Keplerlaan 1, 2200 AG Noordwijk, Netherlands.

⁴ Nicolaus Copernicus Astronomical Center, Bartcyka 18, 00716 Warsaw, Poland.

⁵ Institute of Physical and Chemical Research (RIKEN), 2–1, Hirosawa, Wako, Saitama, 351–0198, Japan.

⁶ Osservatorio Astronomico di Brera, Via Bianchi 46, 23807 Merate (Lc), Italy.

⁷ Osservatorio Astronomico di Roma, Via Frascati 33, 00040 Monteporzio Catone (Roma), Italy.

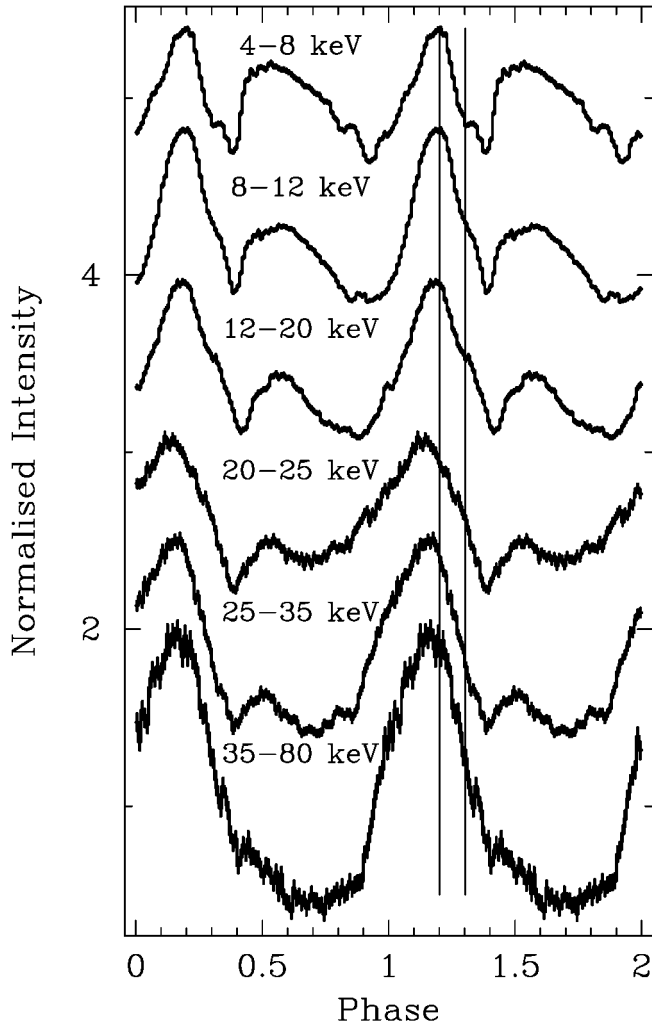


FIG. 1.—Pulse profiles of X0115+63 in six energy bands. The profiles are normalized to unit average and have been shifted vertically by 0.8 for display purposes. Data below (above) 20 keV are from the HPGSPC (PDS). The vertical lines mark the phase interval over which the spectrum of the descending edge of the main pulse has been accumulated. The energy dependence of both the main and soft peaks is apparent.

the NFIs on board the *BeppoSAX* satellite (Boella et al. 1997a) comprise two collimated high-energy detectors, the High-Pressure Gas Scintillation Proportional Counter (HPGSPC; 4–60 keV, FWHM energy resolution of 8% at 10 keV and 5.5% at 20 keV; Manzo et al. 1997) and the Phoswich Detection System (PDS; 15–200 keV, FWHM energy resolution of 24% at 20 keV, and 14% at 60 keV; Frontera et al. 1997).

X0115+63 was observed with the NFIs aboard *BeppoSAX* from March 19, UT 17:05:25 to March 20, 08:42:04. All instruments were operated in their standard configuration. The effective exposure was 3.2 ks for the LECS, 31.4 ks for MECS, 30 ks for HPGSPC, and 16 ks for PDS, which makes use of the rocking collimator technique to monitor the background. The 10–50 keV source flux was $\approx 1.3 \times 10^{-8}$ ergs $\text{cm}^{-2} \text{s}^{-1}$, corresponding to a luminosity of $L_{10-50} \approx 2.5 \times 10^{37} d_4^2$ ergs s^{-1} , where d_4 is the distance in units of 4 kpc (Tamura et al. 1992). The source did not show any significant variability during the observation. In Figure 1 the pulse profiles folded over the best period of $P = 3.6144(1)$ s in six different energy bands are reported. The pulse profile shows the typical double-peaked

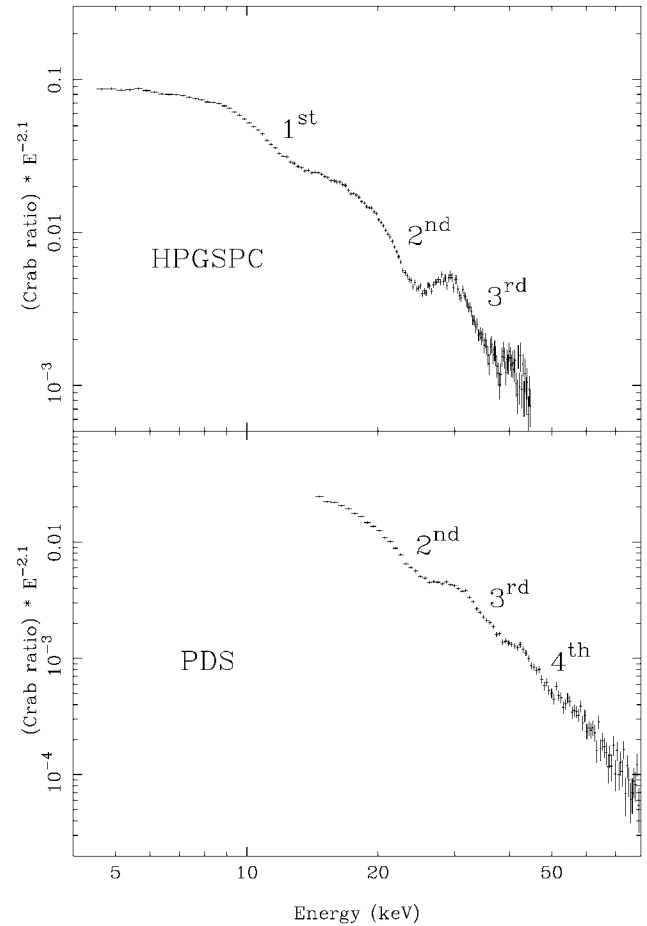


FIG. 2.—Ratio of the HPGSPC (*top*) and PDS (*bottom*) observed count rate spectra with respect to the Crab Nebula count rate spectrum, multiplied by a power law with $\alpha = 2.1$. Spectra correspond to phase 0.2–0.3, the falling edge of the main peak.

structure, already apparent in the *HEAO 1* and *Ginga* data (White, Swank, & Holt 1983; Nagase et al. 1991): a pronounced main peak (phase 0–0.35) followed by a broader and much softer second peak (phase 0.5–0.85). The shape of both peaks is clearly energy dependent.

This Letter concentrates on the high-energy X-ray spectrum (~ 9 –100 keV), based on the HPGSPC and PDS data. In consideration of the strong phase dependence of the cyclotron lines of X0115+63 (Mihara 1995), we accumulated the PHA spectra over 10 pulse phase intervals. Initially, these spectra were divided by the PHA spectrum of the Crab Nebula and multiplied by the spectral shape of the Crab Nebula, a power law with photon index α of 2.1, such that marked spectral features could be spotted in an approximately model- and calibration-independent fashion (Dal Fiume et al. 1999). Dips at ~ 12 , ~ 24 , and ~ 36 , and, possibly, ~ 48 keV were apparent in the spectra from a number of phase intervals. In particular, the spectrum of the descending edge of the main peak (phase of 0.2–0.3), shown in Figure 2, displayed by far the deepest features at ~ 12 , ~ 24 , ~ 36 keV and a clear evidence of a dip at ~ 48 keV. This motivated us to carry out a detailed spectral analysis, with models including multiple harmonic features.

We used the following continuum models to fit the 9–100 keV spectra: (1) the negative and positive power laws exponential (NPEX) model adopted by Mihara (1995) as the standard model for X-ray Pulsars observed with *Ginga*, $f(E) =$

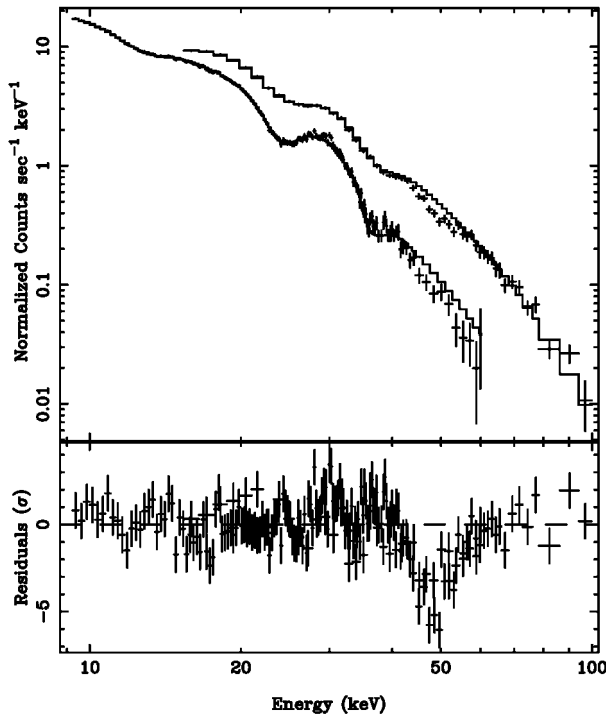


FIG. 3.—The 9–100 keV spectrum of X0115+63 observed by *BeppoSAX* in the descending edge of the main peak. Count rate spectra from the HPGSPC and PDS, together with the best-fit model, which includes the NPEX continuum, and three absorption features are shown in the upper panel. The lower panel shows the residuals in units of σ revealing evidence for an absorption feature at ~ 48 keV.

$(AE^{-\alpha_1} + BE^{+\alpha_2}) \exp(-E/kT)$ and (2) a power law with a high-energy cutoff, $f(E) = AE^{-\alpha} \exp(-E/kT)$. Here $f(E)$ is the photon flux, kT is the e -folding energy, and α is the photon index. Independent of the continuum model used, at least three absorption-like features were required in the fit. These features were introduced in the model(s) as Gaussian filters in absorption, i.e., $G_i(E) = 1 - D_i \exp[-(E - E_i^{\text{cyc}})^2 / (2\sigma_i^2)]$, where E_i^{cyc} , σ_i , and D_i are the centroid energy, width, and depth of each feature. Introducing the third absorption feature at ~ 38 keV (in addition to the first two harmonics at ~ 12 and 24 keV) led to a pronounced improvement in the fit, with the reduced χ_{dof}^2 decreasing from 2.5 (268 degrees of freedom [dof]) to 1.7 (265 dof) in the case of the NPEX model. An F -test shows that the probability of chance improvement is $\sim 10^{-21}$.

The HPGSPC and PDS count spectra of the descending edge of the main peak (pulse phase 0.2–0.3) together with the best-fit model described above are shown in Figure 3 (*upper panel*): an additional feature centered around ~ 48 keV is clearly apparent in the residuals of both the HPGSPC and PDS spectra (Fig. 3, *bottom panel*). This prompted us to introduce a fourth absorption feature, G_4 , in the model; the minimum χ_{dof}^2 decreased to 1.24 (262 dof, NPEX continuum), corresponding to an F -test probability of chance improvement of $\sim 10^{-15}$. Figure 4 shows the unfolded spectrum of X0115+63. Best-fit parameters and equivalent widths are summarized in Table 1. In the same table, best-fit parameters obtained by using the power law with an exponential cutoff are also given.

We also performed a fit with all the line centroids constrained to an integer harmonic spacing. The resulting minimum χ_{dof}^2 is 1.58 (259 dof) for the NPEX model and 1.67 (259 dof) for the power-law plus cutoff model. An F -test gives a probability of

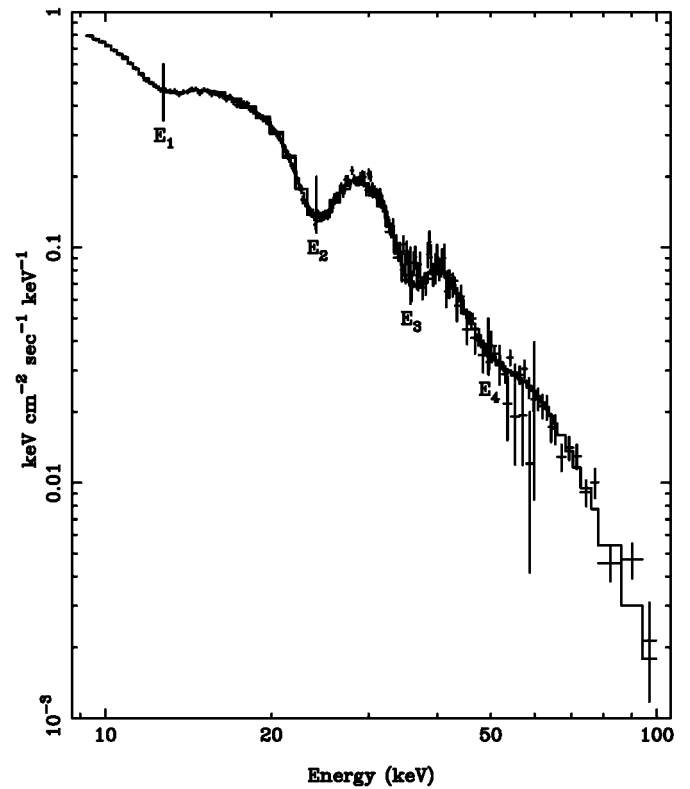


FIG. 4.—Unfolded spectrum of the descending edge of the main peak of X0115+63.

chance improvement for the models with unconstrained line centroids less than 10^{-10} in both cases.

A preliminary analysis of the spectra from other phase intervals also shows significant variations of the line features with the pulse phase confirming previous findings from *Ginga* and *RXTE* (Heindl et al. 1999; Nagase et al. 1991). Variations up to 10% in centroid energy are observed. Three lines are

TABLE 1
BEST-FIT SPECTRAL PARAMETERS^a

PARAMETER	VALUE	
	NPEX	Cutoff Power Law
α_1	1.37 ± 0.05	1.3 ± 0.05
α_2	0.41 ± 0.05	...
kT (keV)	11.0 ± 0.05	17.4 ± 0.5
E_1^{cyc} (keV)	12.74 ± 0.08	12.78 ± 0.08
σ_1 (keV)	1.34 ± 0.25	1.52 ± 0.14
D_1	0.21 ± 0.04	0.23 ± 0.02
EW_1	0.75 ± 0.04	0.87 ± 0.07
E_2^{cyc} (keV)	24.16 ± 0.07	24.0 ± 0.07
σ_2 (keV)	2.11 ± 0.18	1.94 ± 0.11
D_2	0.52 ± 0.02	0.50 ± 0.02
EW_2	2.7 ± 0.07	2.4 ± 0.1
E_3^{cyc} (keV)	35.74 ± 0.35	36.00 ± 0.35
σ_3 (keV)	2.53 ± 0.5	1.98 ± 0.4
D_3	0.46 ± 0.04	0.43 ± 0.04
EW_3	2.8 ± 0.4	2.13 ± 0.3
E_4^{cyc} (keV)	49.5 ± 1.2	49.8 ± 1.4
σ_4 (keV)	6.3 ± 2.3	4.8 ± 2.0
D_4	0.35 ± 0.06	0.3 ± 0.06
EW_4	5.2 ± 1.0	3.4 ± 1.0
χ_{dof}^2 (dof)	1.24 (262)	1.34 (262)

^a Uncertainties at 90% confidence level for a single parameter.

still observed at the descending edge of the soft broad peak, at phase 0.5–0.6, with centroid energies of 11.22 ± 0.3 , 21.69 ± 0.2 , and 32.28 ± 0.5 keV. A comparison with the centroid energies of the three harmonics derived by Heindl et al. (1999) based on *RXTE* data is far from straightforward in consideration of the close but still different pulse phase interval (0.7–0.76) over which their spectrum was accumulated and considering also the different phase of the outburst.

3. CONCLUSIONS

The spectroscopic capabilities of the high-energy instruments (HPGSPC and PDS) on board *BeppoSAX* allowed to us study multiple absorption-like features in the spectrum of the X-ray pulsar transient X0115+63. In particular, four features centered at energies of ~ 12.7 , 24.0, 36, and 50 keV were found in the descending edge of the main peak of the pulse profile. We fitted the line centroids in Table 1 with a simple linear model for the form $E = aN$ (with $N = 1, 2, 3, 4$ and a a free parameter). Unacceptable values of χ^2_{dof} were obtained: 79.3(3) for the power-law plus cutoff model and 71.4(3) for the NPEX model. We conclude that the line centroids reported in Table 1 are not equispaced, for both continuum models. Stated differently, the corresponding harmonic ratios $1 : (1.9 \pm 0.05) : (2.8 \pm 0.05) : (3.9 \pm 0.1)$ are significantly different from the classical values $1 : 2 : 3 : 4$. A closer look at the data reveals that this result can be ascribed entirely to the value of the centroid of the first harmonic. As an example, in the case of a power-law plus cutoff model, the first harmonic is at 12.79 ± 0.05 keV, while a fit to the other three harmonics gives a spacing of 12.02 ± 0.02 keV. Similar results are obtained by using the centroid energies obtained from the NPEX continuum model. We note that, since the first harmonic lies close to the energy interval over which the slope of the X-ray spectrum steepens rapidly, the determination of its centroid energy could be affected by a somewhat inadequate modeling of the continuum. For example, the excess of “shoulder” photons, below the fundamental, as predicted in many theoretical calculations (Isenberg, Lamb, & Wang 1998), may cause the fitted centroid energy of the fundamental to appear higher, therefore causing the harmonic ratios to be somewhat smaller than expected.

It is well known that in strong magnetic fields, the energy spacing of cyclotron harmonics is altered by relativistic effects, i.e., $E_N = m_e c^2 \{ [1 + 2n(B/B_{\text{crit}}) \sin^2 \theta]^{1/2} - 1 \} / \sin^2 \theta$, where m_e is the electron mass, θ is the angle between the photon propagation angle and the magnetic field, and $B_{\text{crit}} = 4.414 \times 10^{13}$ G (see, e.g., Araya & Harding 1996 and Wang, Wasserman, & Lamb 1993). This formula, further corrected for the gravitational redshift, was fit to the centroid energies of the four harmonics observed by *BeppoSAX*. While formally unacceptable [χ^2_{dof} 79.9(2) for the power-law plus cutoff model and 35.7(2) for the NPEX model], the best fit obtained in this way was somewhat better than the simple linear fit.

Despite the uncertainties described above, we conclude that the centroid energies of the four spectral features of X0115+63 are most naturally interpreted in terms of the fundamental, second, third, and fourth harmonics of cyclotron resonant features in a strong magnetic field, taking into account relativistic corrections. This is the first time that four harmonics are observed in the X-ray spectrum of any cosmic source. We find that equivalent widths of the second, third, and fourth harmonics are larger than that of the fundamental, confirming and extending previous results from *Ginga* (Nagase et al. 1991). Such a trend was predicted by Alexander & Mészáros (1989, 1991), who found that two-photon scattering and two-photon emission processes have a major effect in determining the depth of the second and higher harmonics relative to the fundamental. Detailed calculations show that, while the equivalent width of the second harmonic is always larger than the fundamental, this is not necessarily the case for the third (and the fourth) harmonics. In fact, the strength of the third harmonic depends strongly on θ and the optical depth (Isenberg et al. 1998). Comparison of our measured spectra with the ones calculated by Alexander & Mészáros (1991) shows a qualitative agreement. A systematic study of the *BeppoSAX* spectra of X0115+63 as function of pulse phase for different mass accretion rates (i.e., different outburst phases) is currently underway and will be published elsewhere.

The authors wish to thank Milvia Capalbi of the *BeppoSAX* Scientific Data Center and the *BeppoSAX* Mission Director R. C. Butler.

REFERENCES

- Alexander, S. G., & Mészáros, P. 1989, *ApJ*, 344, L1
 ———. 1991, *ApJ*, 372, 565
 Araya, R. A., & Harding, K. A. 1996, *ApJ*, 463, L33
 Boella, G., et al. 1997a, *A&AS*, 122, 299
 ———. 1997b, *A&AS*, 122, 327
 Cusumano, G., Di Salvo, T., Orlandini, M., Piraino, S., Robba, N., & Santangelo, A. 1998, *A&A*, 338, L79
 Dal Fiume, D., et al. 1999, Proc. 32d COSPAR Scientific Assembly, ed. L. Piro & K. Makishima (Amsterdam: Elsevier), in press
 Frontera, F., et al. 1997, *A&AS*, 122, 357
 Grove, J. E., et al. 1995, *ApJ*, 438, L25
 Heindl, W. A., et al. 1999, *ApJ*, 521, L49
 Isenberg, M., Lamb, D. Q., & Wang, J. C. L. 1998, *ApJ*, 505, 688
 Kendziorra, E., et al. 1994, *A&A*, 291, L31
 Kreykenbohm, I., et al. 1998, *A&A*, 341, 141
 Manzo, G., Giarrusso, S., Santangelo, A., Ciralli, F., Fazio, G., Piraino, S., & Segreto, A. 1997, *A&AS*, 122, 341
 Mihara, T. 1995, Ph.D. thesis, Univ. Tokyo
 Nagase, T., et al. 1991, *ApJ*, 375, L49
 Orlandini, M., et al. 1998, *A&A*, 332, 121
 Parmar, A. N., et al. 1997, *A&AS*, 122, 309
 Rappaport, S., Clark, G. W., Cominsky, L., Joss, P. C., & Li, F. 1978, *ApJ*, 224, L1
 Santangelo, A., et al. 1999, Proc. Taormina Integral Workshop, in press
 Tamura, K., Tsunemi, H., Kitamoto, S., Hayashida, K., & Nagase, F. 1992, *ApJ*, 389, 676
 Trümper, J., et al. 1978, *ApJ*, 219, L105
 Unger, S., Roche, P., Negueruela, I., Ringwald, F., Lloyd, C., & Coe, M. 1998, *A&A*, 336, 960
 Wang, J. C. L., Wasserman, I., & Lamb, D. Q. 1993, *ApJ*, 414, 815
 Wheaton, W. A., et al. 1979, *Nature*, 282, 240
 White, N. E., Swank, J. H., & Holt, S. S. 1983, *ApJ*, 270, 711
 Wilson, R., Harmon, B., & Finger, M. 1999, *IAU Circ.* 7116